

ARTICLE

Facet Dependence of Photochemistry of Methanol on Single Crystalline Rutile Titania[†]

Qun-qing Hao^a, Zhi-qiang Wang^a, Xin-chun Mao^b, Chuan-yao Zhou^{a*}, Dong-xu Dai^a, Xue-ming Yang^{a*}*a. State Key Laboratory of Molecular Reaction Dynamics, Dalian Institute of Chemical Physics, Chinese Academy of Science, Dalian 116023, China**b. Center of Interface Dynamics for Sustainability, Institute of Materials, China Academy of Engineering Physics, Chengdu 610200, China*

(Dated: Received on January 11, 2016; Accepted on February 6, 2016)

The crystal phase, morphology and facet significantly influence the catalytic and photocatalytic activity of TiO₂. In view of optimizing the performance of catalysts, extensive efforts have been devoted to designing new sophisticated TiO₂ structures with desired facet exposure, necessitating the understanding of chemical properties of individual surface. In this work, we have examined the photooxidation of methanol on TiO₂(011)-(2×1) and TiO₂(110)-(1×1) by two-photon photoemission spectroscopy (2PPE). An excited state at 2.5 eV above the Fermi level (E_F) on methanol covered (011) and (110) interface has been detected. The excited state is an indicator of reduction of TiO₂ interface. Irradiation dependence of the excited resonance signal during the photochemistry of methanol on TiO₂(011)-(2×1) and TiO₂(110)-(1×1) is ascribed to the interface reduction by producing surface hydroxyls. The reaction rate of photooxidation of methanol on TiO₂(110)-(1×1) is about 11.4 times faster than that on TiO₂(011)-(2×1), which is tentatively explained by the difference in the surface atomic configuration. This work not only provides a detailed characterization of the electronic structure of methanol/TiO₂ interface by 2PPE, but also shows the importance of the surface structure in the photoreactivity on TiO₂.

Key words: TiO₂, Excited state, Two-photon photoemission spectroscopy, Reaction rate of photooxidation

I. INTRODUCTION

Titanium dioxide (TiO₂) is a versatile material in both scientific and technological fields, ranging from surface science, catalysis and photocatalysis to paint, gas sensor and lithium batteries [1–3]. The interaction between adsorbates (molecules or ions) and TiO₂ substrate is the core of the above mentioned scientific issues and functional applications. To a large extent, such adsorbate-substrate interaction is determined by the electronic structure as well as the atomic structure of TiO₂. Therefore, great effort has been devoted to the investigation of the surface dependence of reactivity of TiO₂ [4–6]. The anisotropic chemical reactivity of TiO₂ surfaces has stimulated the fabrication of different TiO₂ nanostructures with specific facets to optimize the performance in the past few years [7, 8]. In surface science and catalysis, there is a conventional criterion

for the reactivity, which says that surfaces with higher percentage of undercoordinated surface atoms are regarded more reactive.

Rutile, the most stable and abundant structure of titania, has attracted tremendous attention in the past decades in surface science and catalysis fields. Rutile (110) surface (Fig.1(b)), one of the most extensively studied metal oxides, has become a prototype for surface chemistry and photochemistry research. The structure of TiO₂(110)-(1×1) has been well understood [2]. On the surface, fivefold coordinated Ti ions (Ti_{5c}) and twofold coordinated bridge O ions (O_b) run alternatively along the [001] azimuth. Reduction leads to the creation of surface oxygen vacancies (O_v) and subsurface Ti interstitials (Ti_{int}) which contribute to the band gap states [9, 10]. In addition to TiO₂(110)-(1×1), the structure of TiO₂(011) surface has also been investigated, though less extensively [11–15]. The most stable phase of TiO₂(011) is reconstructed by (2×1). The atomic structure of TiO₂(011)-(2×1) as suggested by surface X-ray diffraction (SXRD) and density functional theory (DFT) calculations [12, 14] is shown in Fig.1(a). Different from TiO₂(110)-(1×1), inequivalent types of undercoordinated Ti and O atoms exist, namely the valley Ti_{5c}, ridge Ti_{5c}, top O_b and bridge O_b. The top

[†]Part of the special issue for “the Chinese Chemical Society’s 14th National Chemical Dynamics Symposium”.

*Authors to whom correspondence should be addressed. E-mail: chuanyaozhou@dicp.ac.cn, xmyang@dicp.ac.cn, Tel.: +86-411-84695174, FAX: +86-411-84675584

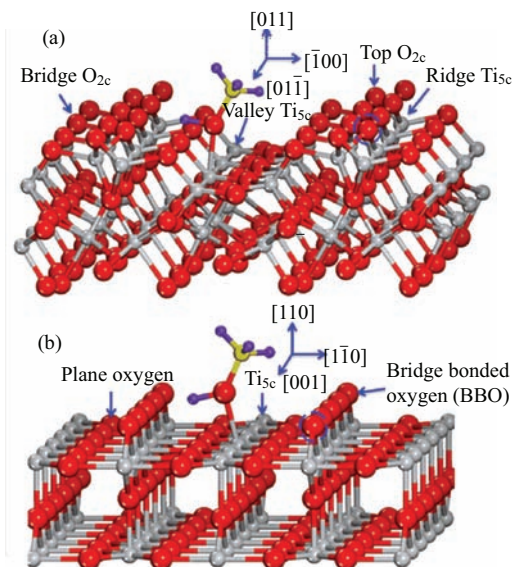


FIG. 1 Structure of rutile $\text{TiO}_2(011)-(2\times 1)$ (a) and $\text{TiO}_2(110)-(1\times 1)$ (b) surfaces. Oxygen and Ti atoms are represented as red and gray spheres, respectively. Surface oxygen vacancies are created by removing the bridge bonded oxygen atoms labeled by dashed circles. Adsorption of methanol on Ti_{5c} sites of these two surfaces are also shown.

O_b atoms display in a zig-zag style, which shade the ridge Ti_{5c} sites severely. Missing of the top O_b atoms creates O_v . All of the Ti sites on $\text{TiO}_2(011)-(2\times 1)$ surface are undercoordinated, while on $\text{TiO}_2(110)-(1\times 1)$, only half of them are unsaturated. According to the conventional criterion, the former should be more reactive than the latter.

The surface dependence of the photoreactivity of rutile has been extensively investigated, especially the low Miller index surfaces such as (110) and (011) [16–24]. Ohno and coworkers reported the selectively photo-assisted deposition of nanoparticles on different surfaces of TiO_2 [20]. Under ultraviolet (UV) irradiation, photooxidation of Pb^{2+} into PbO_2 took place on (011) surface, while photoreduction of Pt^{2+} into Pt occurred on (110) surface. Such a result suggests the rutile (011) surface is more reactive towards photocatalyzed oxidation reaction. Takahashi *et al.* also found (011) is about two times more efficient than (110) in the photocatalyzed oxidation of methylene blue [23]. From the percentage of undercoordinated surface metal ions point of view, these examples seem consistent with the conventional criterion. In fact, researchers have tried to explain the enhanced photocatalytic activity of rutile (011) based on the electronic structures [25]. In this work, Tao and coworkers compared the valence electronic structure of $\text{TiO}_2(011)-(2\times 1)$ and $\text{TiO}_2(110)-(1\times 1)$ using ultraviolet photoelectron spectroscopy (UPS). Finding the binding energy of the band gap state on the (011) surface is 0.34 eV higher than that on (110), they expect the electron trapping and

therefore the electro-hole separation of the former surface is more efficient than the latter.

Most recently, we have reassessed the photoactivity of $\text{TiO}_2(011)-(2\times 1)$ and $\text{TiO}_2(110)-(1\times 1)$ making use of the photocatalyzed oxidation of methanol [26]. Temperature programmed desorption measurements showed the photocatalytic chemical reactions on these two surfaces are the same under identical experimental condition. Methanol molecules adsorbed on Ti_{5c} sites are converted into formaldehyde under ultraviolet (UV) irradiation; released hydroxyl and methyl hydrogen atoms, which transfer to the neighboring O_b sites, generating bridging hydroxyls which experience recombinative desorption as water by abstracting lattice oxygen above 400 K; cross coupling of methoxy and formaldehyde produces methyl formate. Despite the same photocatalyzed oxidation reaction of methanol on $\text{TiO}_2(011)-(2\times 1)$ and $\text{TiO}_2(110)-(1\times 1)$, the reaction rate of the latter is 2.4 times of that of the former. The result suggests the reactivity of $\text{TiO}_2(011)-(2\times 1)$ is lower than $\text{TiO}_2(110)-(1\times 1)$ towards photooxidation reaction, in contrast with previous studies [20, 23]. The contradiction likely comes from the structure of the TiO_2 surface. In Refs.[20, 23], the reactions took place in aqueous, while in our study, the measurements were carried out in ultrahigh vacuum (UHV) environment.

As an extension of our previous study [26], we have studied the photochemistry of methanol on both $\text{TiO}_2(011)-(2\times 1)$ and $\text{TiO}_2(110)-(1\times 1)$ using two-photon photoemission spectroscopy (2PPE). An excited state at 2.5 eV above the Fermi level (E_F) of clean and methanol/ TiO_2 interfaces, which serves as an indicator of surface reduction, has been detected. The properties of this state, for example, the energy level, angular distribution, lifetime and transition dipole moment, have been characterized. The excited resonance signal on both methanol/ TiO_2 interfaces increase with UV light exposure, which corresponds to the reduction of the TiO_2 interface by depositing hydrogen atoms onto the surface during the photooxidation of methanol. Though the photocatalyzed reactions of methanol on both $\text{TiO}_2(011)-(2\times 1)$ and $\text{TiO}_2(110)-(1\times 1)$ are the same, the reaction rate on the latter surface is 11.4 times of that on the former. This work implies the role of surface structure in the photoreactivity of photocatalysts.

II. EXPERIMENTS

All experiments were conducted in a UHV chamber (base pressure better than 5×10^{-11} mbar), which has been described in detail previously [27]. Briefly, a preparation and characterization together with an electron spectroscopy measurement chamber are included in the UHV system. Ar^+ ion source, home-made resistive heater, low energy electron diffraction (LEED) and X-ray photoelectron spectroscopy (XPS) detectors are equipped for sample preparation and characterization respectively. The whole probing chamber is shielded

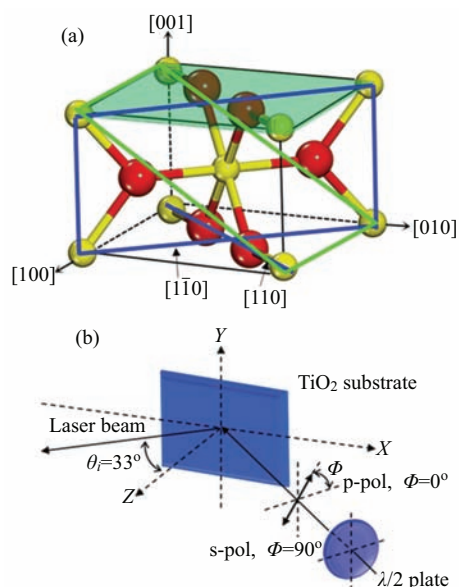


FIG. 2 (a) Unit cell of rutile TiO_2 . The (110) and (011) surfaces are outlined by the blue and green rectangles, respectively. (b) Schematic overview of the experimental geometry. The electric field of the laser can be varied by a half waveplate. For p-polarization (s-polarization), the electric field of the laser lies in the XZ (YZ) plane.

from the earth magnetism by μ -metal. The key element of this apparatus is the hemispherical electron energy analyzer (PHOIBOS 100, SPECS) for photoelectron detection. The energy and angular distribution of photoelectrons are recorded by a two-dimension (2D) CCD camera which facilitates the measurement of the whole photoelectrons within the energy range of interest simultaneously. Therefore, study of the kinetics of the surface reaction becomes feasible. The fundamental output of a tunable oscillator (MaiTai eHP, Spectra-Physics) is adjusted at about 800 nm with a pulse width of about 70 fs. It is converted to the second harmonic (around 400 nm, FWHM=4 nm) and then focused onto the sample (diameter $\approx 100 \mu\text{m}$). The pulse width and average power of the 400 nm laser beam at the sample surface is about 90 fs and 150 mW, respectively. Polarization of the excitation light is rotated through a $\lambda/2$ plate before the lens. The experimental geometry is shown in Fig.2. For p-polarization (s-polarization), the electric field of the laser lies in the horizontal (vertical) plane. In the case of the two-photon (ca. 400 nm) excitation from the TiO_2 interface [28], the first photon excites an electron from below the E_F to above it, and the second photon excites the electron to the vacuum. The energy and angular distribution of the photoelectrons give rise to the 2PPE spectra. Both time-resolved 2PPE (TR-2PPE) and time-dependent 2PPE (TD-2PPE) experiments can be carried out on this instrument. In the TR-2PPE experiment, one can study the ultrafast dynamics of excited electronic states, while TD-2PPE can measure the photochemical kinetics of molecularly

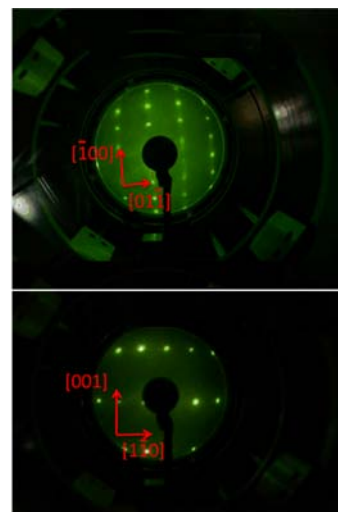


FIG. 3 LEED pattern of rutile $\text{TiO}_2(011)-(2\times 1)$ (top) and $\text{TiO}_2(110)-(1\times 1)$ (bottom) surfaces. Azimuth directions are labeled by arrows. In the 2PPE measurements, the incident planes are the horizontal planes along the $[01\bar{1}]$ and $[1\bar{1}0]$ for $\text{TiO}_2(011)-(2\times 1)$ and $\text{TiO}_2(110)-(1\times 1)$, respectively.

adsorbed surfaces.

TiO_2 samples (Princeton Scientific Corp., 10 mm \times 10 mm \times 1 mm) are mounted on a manipulator with four freedoms (translation along X , Y , Z axes and rotation around the polar axis) and are heated through resistive heating method and cooled by liquid nitrogen. K type thermocouples are glued directly to the TiO_2 surfaces using a ceramic adhesive (Ceramabond 503, Aremco Products, INC) to provide accurate temperature reading. The as received TiO_2 samples are polished on both sides to ensure maximum thermal contact. The samples were cleaned by cycles of Ar^+ sputtering (1 keV, 15 min) and UHV annealing at 850 K (30 min). After this preparation procedure, no contamination could be detected in XPS, and sharp (2 \times 1) and (1 \times 1) LEED patterns were observed for (011) and (110) surface respectively (Fig.3). The preparation history of these two surface studied in the present work was similar.

Methanol (Sigma-Aldridge) was purified by freeze-pump-thaw cycles and introduced onto the TiO_2 surfaces through a home-built, calibrated effusive molecular beam doser at 120 K. A mass spectrometer (SRS, RGA 200) which was shielded by a glass enclosure and differentially pumped was chosen to measure the relative coverage of methanol via TPD method [29]. Temperature was ramped at 2 K/s during all the TPD experiments. Methanol coverage was measured with respect to the corresponding density of Ti_{5c} sites. Here, monolayer (ML) corresponds to 5.2×10^{14} molecules/cm 2 on (110)-(1 \times 1) while, this value is 4.0×10^{14} molecules/cm 2 on (011)-(2 \times 1) [30].

III. RESULTS AND DISCUSSION

Before the adsorption of methanol, the electronic structures of both clean $\text{TiO}_2(011)-(2\times 1)$ and $\text{TiO}_2(110)-(1\times 1)$ are characterized and compared by 2PPE (Fig.4). In the present work, the incident planes are the horizontal planes along the $[01\bar{1}]$ and $[1\bar{1}0]$ for $\text{TiO}_2(011)-(2\times 1)$ and $(110)-(1\times 1)$, respectively (Fig.2 and Fig.3). In accord with our previous studies [31], the work function (defined as the half intensity point of the secondary electron edge) of the clean $\text{TiO}_2(110)-(1\times 1)$ is 5.1 eV, and an excited state at 2.5 eV above the E_F is detected by the 2PPE spectra acquired by p-polarized (p-2PPE) rather than s-polarized light (s-2PPE). The net excited state signal was obtained by subtracting the normalized s-2PPE from the p-2PPE (P-NS in Fig.4(b)). Whereas the 2PPE measurements on $\text{TiO}_2(011)-(2\times 1)$ show some differences compared with $(110)-(1\times 1)$. First of all, the work function is about 0.1 eV higher, although the preparation history of these two surfaces is similar. As the work function reflect the reduction of the surfaces, this result indicates the (110) is easier to reduce than (011), which is consistent with the stronger band gap state signal on the former surface measured by UPS [25]. The most prominent difference comes from the polarization dependence of the excited state. For $\text{TiO}_2(110)-(1\times 1)$, when the incident plane is along $[1\bar{1}0]$ azimuth, the excited state can only be detected by p-polarized, while the s-polarized light is totally “blind” to this state. However, on $\text{TiO}_2(011)-(2\times 1)$ (Fig.4(a)), when the incident plane is along $[01\bar{1}]$ azimuth, s-2PPE is much more pronounced at 5.6 eV (final state energy) than p-2PPE. We have proven the resonance at 5.6 eV is from an excited state in both s-2PPE and p-2PPE. The varied polarization dependence of the excited state on $\text{TiO}_2(011)-(2\times 1)$ and $\text{TiO}_2(110)-(1\times 1)$ suggests different transition dipole moment relative to the distinct surface. The excited states on both surfaces show little angular dependence, suggesting the localized character. In addition, the lifetime of the excited states are too short to measure according to the TR-2PPE using 90 fs light pulse.

The photochemistry of alcohol on $\text{TiO}_2(110)-(1\times 1)$ investigated by 2PPE has been reported by our group in the last several years [28, 32–35]. Figure 5 shows the 2PPE measurements of the 0.5 ML methanol covered $\text{TiO}_2(011)-(2\times 1)$ (a) and $\text{TiO}_2(110)-(1\times 1)$ (b), after the methanol/ TiO_2 interfaces have been exposed to the 2PPE probe light for more than 200 and 2000 s in the case of (011) and (110) surface respectively. Compared with the bare surfaces, the 2PPE spectra on both methanol covered TiO_2 interfaces showed similar angular distribution, lifetime, decrease of work function and increase of the overall intensity [36]. The excited states become much more pronounced, and moreover, no change in the light polarization dependence of the 2PPE has been detected.

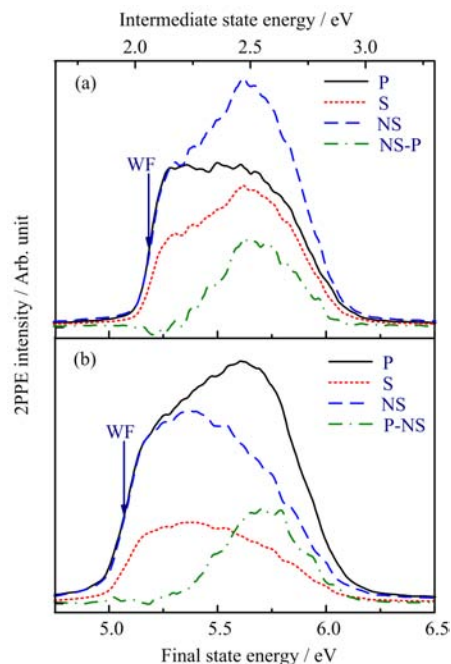


FIG. 4 Typical 2PPE spectra for the clean (a) $\text{TiO}_2(011)-(2\times 1)$ and (b) $\text{TiO}_2(110)-(1\times 1)$ surfaces respectively. The spectra were measured with both p-polarized (P) and s-polarized (S) light with a photon energy of 3.10 eV. For comparison, S was normalized to P at the secondary electron signal edge. NS-P or P-NS denotes the difference spectra. The signal was integrated from -5° to $+5^\circ$. Energies are measured with respect to E_F ; those in the bottom axis represent final state, after absorption of two photons, while those in the top X-axis refer to the intermediate state, before absorption of the second photon. Work function (WF) is labeled by the arrow at the middle of the secondary electron edge. The incident planes are the horizontal planes along the $[01\bar{1}]$ and $[1\bar{1}0]$ for $\text{TiO}_2(011)-(2\times 1)$ and $\text{TiO}_2(110)-(1\times 1)$, respectively.

TD-2PPE showed the evolution of the electronic structure as a function of light irradiation on both methanol covered $\text{TiO}_2(011)-(2\times 1)$ and $\text{TiO}_2(110)-(1\times 1)$ (Fig.6). During the TD-2PPE measurements, the probe light was directed to the methanol/ TiO_2 interface without any interruption, and the 2PPE spectra were collected every second. The irradiation dependence of the excited resonance signal suggests the occurrence of photoinduced chemistry on the methanol/ TiO_2 interfaces. The excited resonance signal on methanol/ $\text{TiO}_2(110)-(1\times 1)$ (Fig.6(b)) increased by 68% when the light exposure time was increased from zero to 200 s. While on methanol/ $\text{TiO}_2(011)-(2\times 1)$ (Fig.6(a)), this signal was doubled when the irradiation time reached 2000 s. It should be noted in Fig.6, the 2PPE spectra were acquired by p-polarized and s-polarized light on $\text{TiO}_2(110)-(1\times 1)$ and $\text{TiO}_2(011)-(2\times 1)$ interface respectively to maximize the excited resonance signal.

Since the energy level, angular distribution, lifetime

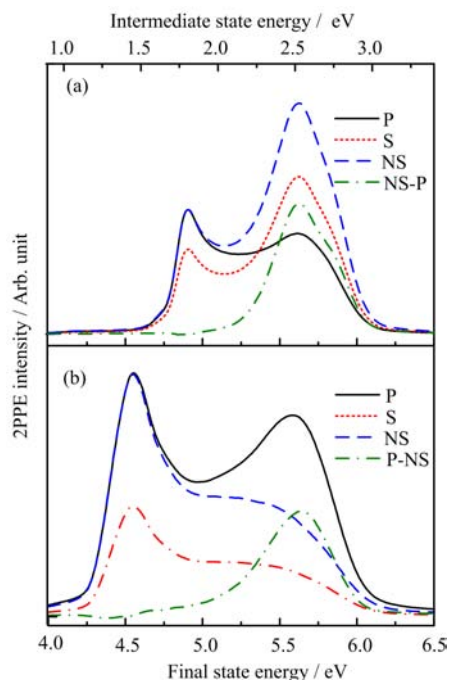


FIG. 5 Typical 2PPE spectra for the 0.5 ML methanol covered (a) $\text{TiO}_2(011)-(2\times 1)$ and (b) $\text{TiO}_2(110)-(1\times 1)$ surfaces respectively. The signal was integrated from -5° to $+5^\circ$. Energies are measured with respect to E_F . Before the acquisition of these spectra, the $\text{TiO}_2(011)-(2\times 1)$ and $\text{TiO}_2(110)-(1\times 1)$ interfaces has been exposed to the 2PPE light for more than 2000 and 200 s respectively.

and the light polarization dependence of the excited state are similar, it is natural for one to think the origins of the excited states on both clean and adsorbated covered TiO_2 are the same. In our most recently combined 2PPE and density functions theory (DFT) calculations study [31], we have demonstrated the band gap state and the excited state at about 2.5 eV above the E_F of $\text{TiO}_2(110)-(1\times 1)$ result from the splitting of the d orbitals of Ti^{3+} in the distorted octahedral field. This means both the band gap state and the excited state we discuss here are indicators for reduction of TiO_2 surface. And on $\text{TiO}_2(011)-(2\times 1)$, we have proven this conclusion is still correct (data are not shown). The irradiation dependence of the electronic structure on methanol/ TiO_2 interfaces is consistent with our interpretation to the excited state on clean TiO_2 surfaces. As revealed by TPD studies, methanol on both $\text{TiO}_2(011)-(2\times 1)$ and $\text{TiO}_2(110)-(1\times 1)$ experienced photocatalyzed oxidation under UV exposure, releasing hydrogen atoms onto the surface bridge oxygen atoms to produce hydroxyls. Similar to the creation of surface O_v and subsurface Ti interstitials, hydroxylation is another way to reduce the TiO_2 surface [29]. Therefore, as methanol molecules are split by UV light, more and more hydrogen atoms are deposited onto the TiO_2 interface where more and more Ti^{3+} ions are generated. Consequently, the density of

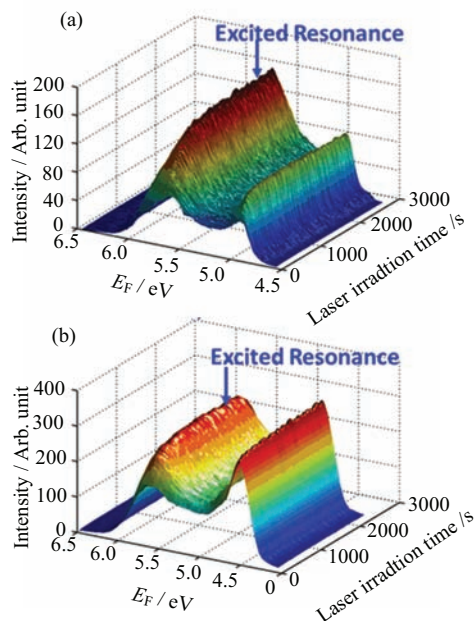


FIG. 6 2PPE spectra for the 0.5 ML methanol covered (a) $\text{TiO}_2(011)-(2\times 1)$ and (b) $\text{TiO}_2(110)-(1\times 1)$ as a function of the probe laser irradiation time. Most of the laser parameters (center wavelength, band width and power) in the two experimental measurements were exactly the same except the polarization. On $\text{TiO}_2(110)-(1\times 1)$ and $\text{TiO}_2(011)-(2\times 1)$ interfaces, 2PPE spectra were acquired by p-polarized and s-polarized light respectively to maximize the excited resonance signal. The signal in these spectra was integrated from -5° to $+5^\circ$. The energies were measured with respect to the Fermi level.

states (DOS) of both the band gap state and the excited state become intensified. As demonstrated, the 2PPE measured excited resonance signal scales linearly with the coverage of surface hydroxyls on clean TiO_2 surface [31]. Furthermore, on adsorbate (methanol or water) covered TiO_2 , the excited resonance signal is also proportional to the density of coadsorbed hydroxyls (data not shown). Therefore, the increase of the excited resonance signal during the photochemistry of methanol in fact reflects the accumulation of surface hydroxyls on TiO_2 interface.

Since the 2PPE measured excited resonance signal is an indicator of the density of hydroxyls on TiO_2 interface, it provides a fingerprint to trace the kinetics of the photocatalyzed oxidation of methanol on TiO_2 . Figure 7 displays the time-dependent excited resonance together with the fitting by a fractal-like model [28, 32, 33]. On $\text{TiO}_2(011)-(2\times 1)$, the signal was integrated between 5.25 and 6.20 eV from s-2PPE (Fig.6(a)), whereas on $\text{TiO}_2(110)-(1\times 1)$, the excited resonance was accumulated in a span of 5.00–6.25 eV from p-2PPE (Fig.6(b)). Although the photocatalytic chemical reactions of methanol on both $\text{TiO}_2(011)-(2\times 1)$ and $\text{TiO}_2(110)-(1\times 1)$ are similar, the reaction rate, however, differs dramatically from each other. From Fig.7,

TABLE I Comparison of the light source parameters in the 2PPE and TPD studies.

Methods	Light source parameters				
	Wavelength/nm	Repetition rate/Hz	Pulse width/fs	Average power/mW	Diameter/mm
2PPE	400	8×10^7	90	150	0.1
TPD	400	1×10^3	~ 100	400	6.0

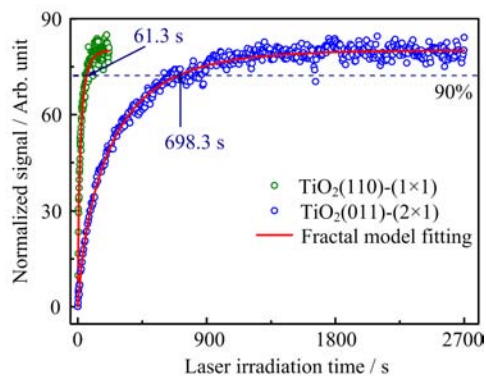


FIG. 7 Normalized time dependent signal of the excited resonance feature of 0.5 ML methanol covered $\text{TiO}_2(011)-(2 \times 1)$ (blue circle) and $\text{TiO}_2(110)-(1 \times 1)$ (olive circle) and the fractal-like kinetics model fitting (red line). On $\text{TiO}_2(011)-(2 \times 1)$, the signal was integrated between 5.25 and 6.20 eV from s-2PPE (Fig.6(a)), whereas on $\text{TiO}_2(110)-(1 \times 1)$, the excited resonance was accumulated in a span of 5.00–6.25 eV from p-2PPE (Fig.6(b)).

one can see that it takes 61.3 s for the excited resonance signal on $\text{TiO}_2(110)-(1 \times 1)$ to rise to 90% of the maximum signal level, while on $\text{TiO}_2(011)-(2 \times 1)$, it costs 698.3 s, showing a 11.4 times difference from the reaction rate. The photocatalyzed oxidation of methanol on $\text{TiO}_2(011)-(2 \times 1)$ is less efficient than on $\text{TiO}_2(110)-(1 \times 1)$, in accord with our previous TPD investigation [26]. In the same work, our DFT calculations provided some interpretation to the difference of the photocatalyzed oxidation of methanol on these two TiO_2 surfaces. Methanol molecules are converted into methoxy before further photooxidation to formaldehyde, and the cleavage of C–H bond on both $\text{TiO}_2(011)-(2 \times 1)$ and $\text{TiO}_2(110)-(1 \times 1)$ are the rate determining step during the photooxidation of methanol. Nevertheless, due to the corrugated structure, the distance between the nearest surface oxygen atoms and the methyl hydrogen of methoxy intermediate on $\text{TiO}_2(011)-(2 \times 1)$ is 0.3 Å larger than that on $\text{TiO}_2(110)-(1 \times 1)$, leading to the 0.2 eV higher reaction barrier of break of the C–H bond. Anisotropic bulk charge transportation along different directions might also be a factor which affects the surface dependence of photochemistry [24].

Though both our 2PPE and TPD [26] measurements suggest $\text{TiO}_2(011)-(2 \times 1)$ is less efficient than $\text{TiO}_2(110)-(1 \times 1)$ towards the photooxidation of methanol, the relative photoreactivity obtained in these two studies are different. In the present 2PPE work, the

reaction rate on $\text{TiO}_2(110)-(1 \times 1)$ is 11.4 times faster, while the TPD results show a 2.4 times of difference. The discrepancy possibly originates from the different light source chosen in these two studies (Table I). The flux (number of photons per unit area per second) in the TPD experiments is about 60 times of that in the 2PPE measurements. It is well known the light flux affects the dynamics of the charge carriers significantly [37]. It has also been proven the charge carrier transportation in TiO_2 is anisotropic [38]. Therefore, it is possible the dependence of the charge carrier kinetics and dynamics on the light flux along [110] and [011] direction are different, which might lead to the discrepancy in the relative photoreactivity under different light irradiation condition. However, in both studies, we have found $\text{TiO}_2(011)-(2 \times 1)$ is inferior to $\text{TiO}_2(110)-(1 \times 1)$ towards the photooxidation of methanol.

Our previous [26] and present investigations of the photooxidation of methanol on $\text{TiO}_2(011)-(2 \times 1)$ and $\text{TiO}_2(110)-(1 \times 1)$ show inconsistency with others' work which suggest $\text{TiO}_2(011)$ is more efficient towards photooxidation reactions than $\text{TiO}_2(110)$ [20, 23]. The discrepancy likely originates from the structure of the TiO_2 photocatalyst. It is worth noting the photoreactivity tested in Ref.[20, 23] is in aqueous environment which often alters the surface structure dramatically, causing it difficult to establish the correlation between activity and surface structure from an atomic level [39]. To avoid such complexity, photocatalysis studied in UHV condition is necessary. Since the surface structure in vacuum can be well characterized, and submonolayer adsorbates usually change the surface structure slightly [40].

IV. CONCLUSION

We have investigated the electronic structure of clean and methanol covered $\text{TiO}_2(011)-(2 \times 1)$ and $\text{TiO}_2(110)-(1 \times 1)$. An excited state at 2.5 eV above the E_F on all the four TiO_2 interfaces (clean and methanol covered (011) and (110)) studied here has been detected. The energy level, angular distribution and lifetime of this excited state are similar on both (110) and (011) interfaces. However, the transition dipole moment shows different configuration relative to the interfaces. The excited state is an indicator of reduction of TiO_2 interface. Irradiation dependence of the excited resonance signal during the photochemistry of methanol on $\text{TiO}_2(011)-(2 \times 1)$ and $\text{TiO}_2(110)-(1 \times 1)$ is attributed to the reduction of the interfaces by depositing hydrogen

atoms. The reaction rate of photooxidation of methanol on $\text{TiO}_2(110)-(1 \times 1)$ is about 11.4 times faster than that on $\text{TiO}_2(011)-(2 \times 1)$, which is tentatively explained by the difference in the surface atomic configuration.

This work not only provides a detailed characterization of the electronic structure of methanol/ TiO_2 interface by 2PPE, but also shows the importance of the surface structure in the photoreactivity on TiO_2 . Anisotropy of the surface properties are attracting more and more attention. For example, charge separation in photocatalysis has been successfully realized by constructing heterostructures with different facets [41]. Therefore, studying the properties of individual surface and the dependence on the surfaces are desirable.

V. ACKNOWLEDGMENTS

This work was supported the Natural Science Foundation of Liaoning Province (No.2015020242), the National Natural Science Foundation of China (No.21203189 and No.21573225), and the State Key Laboratory of Molecular Reaction Dynamics (No.ZZ-2014-02).

- [1] A. L. Linsebigler, G. Q. Lu, and J. T. Yates, *Chem. Rev.* **95**, 735 (1995).
- [2] U. Diebold, *Surf. Sci. Rep.* **48**, 53 (2003).
- [3] Q. Guo, C. Zhou, Z. Ma, Z. Ren, H. Fan, and X. Yang, *Chem. Soc. Rev.* DOI: 10.1039/c5cs00448, (2015).
- [4] C. Xu, W. Yang, Q. Guo, D. Dai, M. Chen, and X. Yang, *J. Am. Chem. Soc.* **135**, 10206 (2013).
- [5] C. Xu, W. Yang, Q. Guo, D. Dai, M. Chen, and X. Yang, *J. Am. Chem. Soc.* **136**, 602 (2014).
- [6] A. Vittadini, A. Selloni, F. P. Rotzinger, and M. Gratzel, *Phys. Rev. Lett.* **81**, 2954 (1998).
- [7] H. G. Yang, C. H. Sun, S. Z. Qiao, J. Zou, G. Liu, S. C. Smith, H. M. Cheng, and G. Q. Lu, *Nature* **453**, 638 (2008).
- [8] G. Liu, H. G. Yang, J. Pan, Y. Q. Yang, G. Q. Lu, and H. M. Cheng, *Chem. Rev.* **114**, 9559 (2014).
- [9] V. E. Henrich, G. Dresselhaus, and H. J. Zeiger, *Phys. Rev. Lett.* **36**, 1335 (1976).
- [10] S. Wendt, P. T. Sprunger, E. Lira, G. K. H. Madsen, Z. S. Li, J. O. Hansen, J. Matthiesen, A. Blekinge-Rasmussen, E. Laegsgaard, B. Hammer, and F. Besenbacher, *Science* **320**, 1755 (2008).
- [11] T. J. Beck, A. Klust, M. Batzill, U. Diebold, C. Di Valentin, and A. Selloni, *Phys. Rev. Lett.* **93**, 036104 (2004).
- [12] X. Torrelles, G. Cabailh, R. Lindsay, O. Bikondoa, J. Roy, J. Zegenhagen, G. Teobaldi, W. A. Hofer, and G. Thornton, *Phys. Rev. Lett.* **101**, 185501 (2008).
- [13] S. E. Chamberlin, C. J. Hirschmugl, H. C. Poon, and D. K. Saldin, *Surf. Sci.* **603**, 3367 (2009).
- [14] X. Q. Gong, N. Khorshidi, A. Stierle, V. Vonk, C. Ellinger, H. Dosch, H. Z. Cheng, A. Selloni, Y. B. He, O. Dulub, and U. Diebold, *Surface Science* **603**, 138 (2009).
- [15] T. Woolcot, G. Teobaldi, C. L. Pang, N. S. Beglitis, A. J. Fisher, W. A. Hofer, and G. Thornton, *Phys. Rev. Lett.* **109**, 156105 (2012).
- [16] P. A. M. Hotsenpiller, J. D. Bolt, W. E. Farneth, J. B. Lowekamp, and G. S. Rohrer, *J. Phys. Chem. B* **102**, 3216 (1998).
- [17] J. B. Lowekamp, G. S. Rohrer, P. A. M. Hotsenpiller, J. D. Bolt, and W. E. Farneth, *J. Phys. Chem. B* **102**, 7323 (1998).
- [18] T. Sugiura, S. Itoh, T. Ooi, T. Yoshida, K. Kuroda, and H. Minoura, *J. Electroanal. Chem.* **473**, 204 (1999).
- [19] A. Tsujiko, T. Kisumi, Y. Magari, K. Murakoshi, and Y. Nakato, *J. Phys. Chem. B* **104**, 4873 (2000).
- [20] T. Ohno, K. Sarukawa, and M. Matsumura, *New J. Chem.* **26**, 1167 (2002).
- [21] A. Y. Ahmed, T. A. Kandiel, T. Oekermann, and D. Bahnemann, *J. Phys. Chem. Lett.* **2**, 2461 (2011).
- [22] Y. Nakabayashi and Y. Nosaka, *J. Phys. Chem. C* **117**, 23832 (2013).
- [23] H. Takahashi, R. Watanabe, Y. Miyauchi, and G. Mizutani, *J. Chem. Phys.* **134**, 154704 (2011).
- [24] T. Luttrell, S. Halpegamage, J. Tao, A. Kramer, E. Sutter, and M. Batzill, *Sci. Rep.* **4**, 4043 (2014).
- [25] J. G. Tao and M. Batzill, *J. Phys. Chem. Lett.* **1**, 3200 (2010).
- [26] X. Mao, Z. Wang, X. Lang, Q. Hao, B. Wen, D. Dai, C. Zhou, L. M. Liu, and X. Yang, *J. Phys. Chem. C* **119**, 6121 (2015).
- [27] Z. F. Ren, C. Y. Zhou, Z. B. Ma, C. L. Xiao, X. C. Mao, D. X. Dai, J. LaRue, R. Cooper, A. M. Wodtke, and X. M. Yang, *Chin. J. Chem. Phys.* **23**, 255 (2010).
- [28] C. Zhou, Z. Ma, Z. Ren, A. M. Wodtke, and X. Yang, *Energy Environ. Sci.* **5**, 6833 (2012).
- [29] X. C. Mao, X. F. Lang, Z. Q. Wang, Q. Q. Hao, B. Wen, Z. F. Ren, D. X. Dai, C. Y. Zhou, L. M. Liu, and X. M. Yang, *J. Phys. Chem. Lett.* **4**, 3839 (2013).
- [30] J. Tao, Q. Cuan, X. Q. Gong, and M. Batzill, *J. Phys. Chem. C* **116**, 20438 (2012).
- [31] Z. Wang, B. Wen, Q. Hao, L. M. Liu, C. Zhou, X. Mao, X. Lang, W. J. Yin, D. Dai, A. Selloni, and X. Yang, *J. Am. Chem. Soc.* **137**, 9146 (2015).
- [32] C. Y. Zhou, Z. F. Ren, S. J. Tan, Z. B. Ma, X. C. Mao, D. X. Dai, H. J. Fan, X. M. Yang, J. LaRue, R. Cooper, A. M. Wodtke, Z. Wang, Z. Y. Li, B. Wang, J. L. Yang, and J. G. Hou, *Chem. Sci.* **1**, 575 (2010).
- [33] C. Zhou, Z. Ma, Z. Ren, X. Mao, D. Dai, and X. Yang, *Chem. Sci.* **2**, 1980 (2011).
- [34] Z. Ma, Q. Guo, X. Mao, Z. Ren, X. Wang, C. Xu, W. Yang, D. Dai, C. Zhou, H. Fan, and X. Yang, *J. Phys. Chem. C* **117**, 10336 (2013).
- [35] Z. B. Ma, C. Y. Zhou, X. C. Mao, Z. F. Ren, D. X. Dai, and X. M. Yang, *Chin. J. Chem. Phys.* **26**, 1 (2013).
- [36] Z. Wang, Q. Hao, X. Mao, C. Zhou, Z. Ma, Z. Ren, D. Dai, and X. Yang, *Chin. J. Chem. Phys.* **28**, 123 (2015).
- [37] Y. Tamaki, A. Furube, M. Murai, K. Hara, R. Katoh, and M. Tachiya, *Phys. Chem. Chem. Phys.* **9**, 1453 (2007).
- [38] L. Thulin and J. Guerra, *Phys. Rev. B* **77**, 195112 (2008).
- [39] U. Aschauer and A. Selloni, *Phys. Rev. Lett.* **106**, 166102 (2011).
- [40] R. S. de Armas, J. Oviedo, M. A. San Miguel, and J. F. Sanz, *J. Phys. Chem. C* **111**, 10023 (2007).
- [41] R. Li, F. Zhang, D. Wang, J. Yang, M. Li, J. Zhu, X. Zhou, H. Han, and C. Li, *Nat. Commun.* **4**, 1432 (2013).